# Research and Development of a Pulsed Plasma Thruster in Osaka University

**IEPC-2005-106**

*Presented at the 29th International Electric Propulsion Conference, Princeton University, October 31 – November 4, 2005*

Toshiaki Edamitsu*, Hirofumi Asakura*, Akinori Matsumoto* and Hirokazu Tahara†
*Graduate School of Engineering Science, Osaka University, Toyonaka, Osaka 560-8531, JAPAN*

**Abstract: In Osaka University, PPTs have been studied since 2003 in order to understand physical phenomena and improve thrust performances with both experiments and numerical simulations. In preliminary studies with a coaxial electrothermal PPT with a cavity of a tubular propellant, basic performance characteristics and energy balance in the discharge circuit were understood. An electrothermal PPT with a side-fed propellant feeding mechanism achieved a total impulse of 3.6 Ns with a repetitive 10000-shot operation. An unsteady numerical simulation showed the existence of considerable amount of ablation delaying to the discharge. However, it was also shown that this phenomenon should not be regarded as the "late time ablation" for electrothermal PPTs. It is also shown by an experiment that a longer nozzle does not have good benefit-to-size ratio. An electrothermal PPT with multiple cavities induced with an igniter as a substitute for the propellant feeding mechanism to use a large amount of propellant was proposed, and the PPT showed a lower decreasing rate of impulse bit in a repetitive operation than a conventional PPT. A preliminary test of a PPT aiming to utilize both the electrothermal and electromagnetic acceleration was also carried out.**

## I. Introduction

PULSED plasma thrusters (PPTs) are expected to be used as a thruster for a small satellite. The PPT has some features superior to other kinds of electric propulsion. It has no sealing part, simple structure and high reliability, which are benefits of using a solid propellant, mainly Teflon® (poly-tetrafluoroethylene: PTFE). However, performances of PPTs are generally low compared with other electric thrusters[1].

In Osaka University, the PPT has been studied since 2003 in order to understand physical phenomena and improve thrust performances with both experiments and numerical simulations. We mainly studied electro-thermal-acceleration-type PPTs, which generally had higher thrust-to-power ratios (impulse bit per unit initial energy stored in capacitors) and higher thrust efficiencies than electromagnetic-acceleration-type PPTs. Although the electrothermal PPT has lower specific impulse than the electromagnetic PPT, the low specific impulse is not a significant problem as long as the PPT uses solid propellant, because there is no tank nor valve for liquid or gas propellant which would be a large weight proportion of a thruster system.

This paper mainly explains studies with 1) a preliminary electrothermal PPT using a tubular propellant, 2) an electrothermal PPT with a side-fed propellant feeding mechanism, 3) an electrothermal PPT with multiple cavities induced with an igniter as a substitute for the propellant feeding mechanism to use a large amount of propellant, and 4) a PPT aiming to utilize the electrothermal acceleration as well as the electromagnetic acceleration with parallel electrodes, sidewalls and nozzle.

* Graduate Student, Mechanical Science and Bioengineering, edamitsu@arl.me.es.osaka-u.ac.jp.
† Associate Professor, AIAA member, Mechanical Science and Bioengineering, tahara@me.es.osaka-u.ac.jp.

## II. Thrust Stand with a Perpendicular Pendulum

Figure 1 shows a thrust stand in a vacuum chamber for a precise measurement of an impulse bit, which is used in measurements without preliminary studies. The PPT and capacitors are mounted on the pendulum, which rotates around fulcrums of two knife edges without friction. The displacement of the pendulum is detected by an eddy-current-type gap sensor (non-contacting micro-displacement meter) near the PPT, which resolution is about ±0.5 μm. The electromagnetic damper is used to suppress mechanical noises and to decrease quickly the amplitude for the next measurement after firing the PPT. It is useful for a sensitive thrust stand because it is non-contacting. The damper consists of a permanent magnet fixed to the pendulum and two coils fixed to the supporting stand. The control circuit differentiates the output voltage of the displacement sensor and supplies the current proportional to the differentiated voltage to the coil. Accordingly, the damper works as a viscosity resistor. The damper is turned off just before firing the PPT for measurements without damping, and turned on after the measurement to prepare for the next measurement. Figure 2 shows a typical signal of displacement in a measurement of impulse bit.

Sensitiveness of the thrust stand is variable by changing the weight mounted on the top of the pendulum as shown in Fig. 3.

A calibration of the thrust stand is carried out by collisions of balls to the pendulum with various balls from various distances corresponding 15-1400 μNs.

Pressure in the vacuum chamber is kept at approximately $4\times10^{-3}$ Pa under operations.

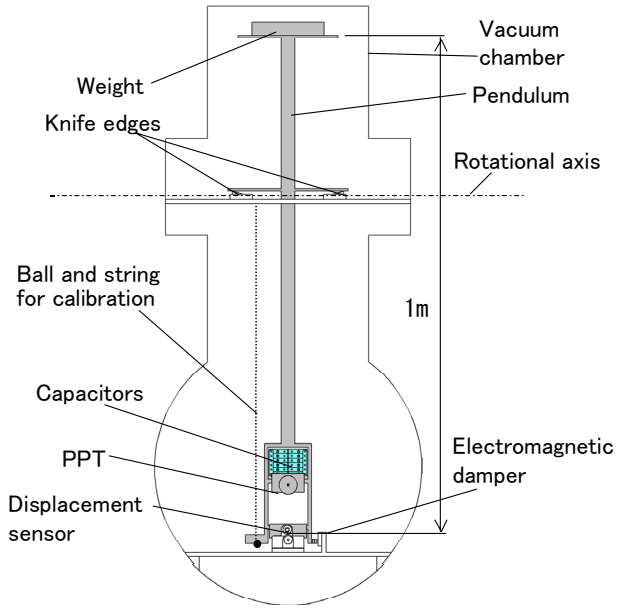


**Figure 1. Thrust stand.**

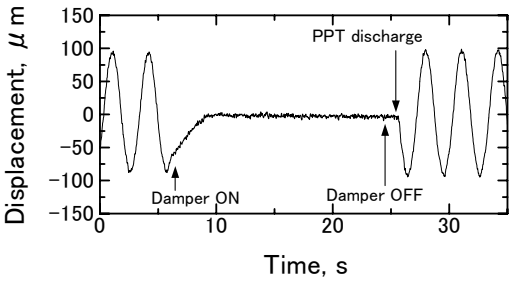


**Figure 2. Typical signal of displacement in a measurement of impulse bit.**

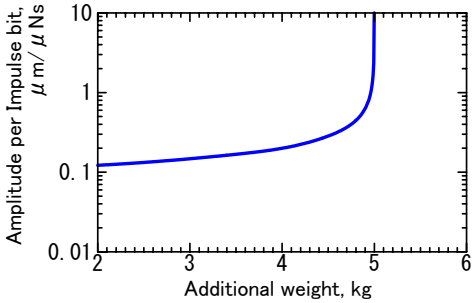


**Figure 3. Sensitiveness of thrust stand vs top weight.**

## III. Preliminary Electrothermal Pulsed Plasma Thruster

### A. Electrothermal PPT for preliminary study

Figure. 4 shows a schematic of coaxial electrothermal PPT with a cavity of a tubular propellant for preliminary studies[2, 3]. The PPT has an anode inside the tube and a divergent nozzle as a cathode with half-angle of 20 degrees and length of 20 mm. The anode and the cathode are made of tungsten and stainless steel, respectively. The distance between the anode and the cathode is equal to the cavity length. The diameter of the cavity is 3 mm, which was designed smaller than that of conventional electrothermal PPTs [4] in order that the pressure in the cavity would rise more highly. In addition, electromagnetic acceleration is also expected due to divergence of current in the cathode

nozzle. The cavity length is variable by varying the position of the anode. A discharge is initiated by an igniter mounted in the nozzle. Figure 5 shows the photograph of the firing PPT.

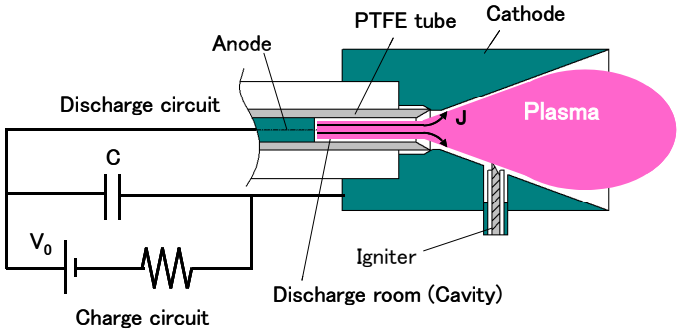


**Figure 4. Coaxial electrothermal PPT for preliminary experiments.**

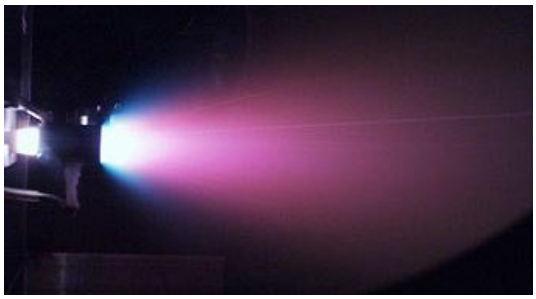

**Figure 5. Photograph of firing PPT (PTFE, cavity length: 14 mm, Stored energy=21.4J).**

## B. Energy efficiencies and equivalent plasma resistance

In the whole discharge system including plasma, there are various energy losses [5] as shown Fig. 6. In this study, we estimated the thrust efficiency $\eta_t$, the transfer efficiency $\eta_{tran}$, and the acceleration efficiency $\eta_{acc}$.[2]

$$\eta_{tran} = E_{in} / E_0 \tag{1}$$

$$\eta_{acc} = E_t / E_{in} \tag{2}$$

$$\eta_t = E_t / E_0 = \eta_{tran}\eta_{acc} \tag{3}$$

where $E_t$ is thrust energy, $E_0$ initial energy stored in the capacitors and $E_{in}$ energy supplied into the plasma. Considering conservation of energy in a discharge, the supplied energy is written as follows:

$$E_{in} = E_0 - \int (R_{tran} + R_C) J^2 dt = \int R_p J^2 dt + \int \frac{\dot{L}_p}{2} J^2 dt \tag{4}$$

where $R$ is direct-current resistance, and subscrips $p$, tran and $C$ represent plasma, transmission lines including electrodes, and capacitors, respectively. $J$ is the discharge current. $R_C$ is generally called the equivalent series resistance (ESR) of the capacitors. In the right-hand side of Eq. (4), the first term and the second term are energies used for the electrothermal and electromagnetic accelerations, respectively. Then, equivalent plasma resistance is defined as:

$$R_{p,eq} \equiv \frac{\int \left(R_p + \dot{L}_p/2\right) J^2 dt}{\int J^2 dt} = \frac{E_{in}}{\int J^2 dt} \tag{5}$$

The transfer efficiency is as follows using this equivalent plasma resistance:

$$\eta_{tran} \equiv \frac{E_{in}}{E_0} = \frac{1}{1 + (R_{tran} + R_C)/R_{p,eq}} \tag{6}$$

The thrust efficiency is estimated by the measurements of the impulse bit and mass loss per shot. The transfer efficiency is estimated by the measurement of discharge circuit with the frequency response method.[2] And the acceleration efficiency is calculated from Eq. (3).

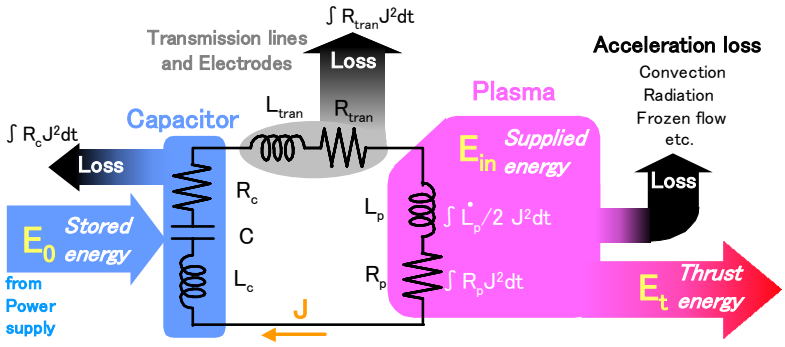


**Figure 6. Energy flow in the discharge circuit including plasma.**

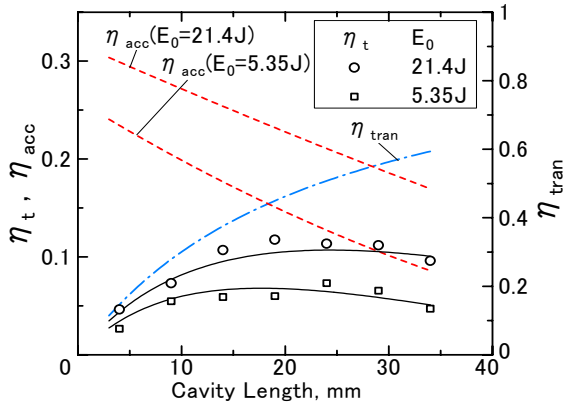


**Figure 7. Efficiencies vs cavity length.**

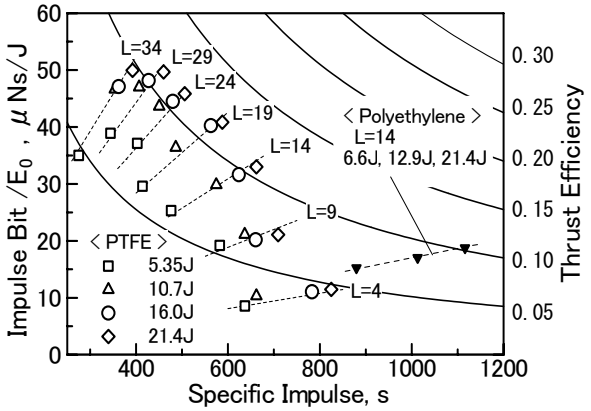


**Figure 8. Impulse bit per unit stored energy vs specific impulse.**

### C. Effects of initial stored energy, cavity length and material on performances.

The energy efficiencies are plotted versus the cavity length in Fig. 7. The transfer efficiency increases with the cavity length. The acceleration efficiency is higher for shorter cavity length. That is, the thrust efficiency falls mainly by the transmission loss if the cavity length is short, and it falls mainly by the acceleration loss if the cavity length is long. As a result, in each stored energy, there is an optimum cavity length between 14 mm and 29 mm for thrust efficiency. This PPT achieved thrust efficiencies of 10-12% at 21.4 J and 6-7% at 5.35 J at cavity lengths between 14 mm and 29 mm.

Figure 8 shows the impulse bit per unit stored energy versus the specific impulse. It is shown that this PPT achieves the wide-range performance by varying the cavity length, and that the performance approaches that of electromagnetic-acceleration-type PPT with decreasing cavity length.

Polyethylene (PE) tube is tested as a propellant at a cavity length of 14 mm. Using the PE tube, the specific impulse significantly increases, because the hydrogen in the PE is lighter than fluorine in the PTFE and the sound speed of PE is faster than that of PTFE.[1] However, the impulse bit per unit stored energy with the PE tube is lower than that with PTFE. As a result, the thrust efficiency with PE is approximately the same as that with PTFE. However, discharges without an ignition are observed. It is caused by the charring on the surface of the PE tube. Any charring is not observed on the Teflon surface.

### D. Improvement of the discharge circuit

After the above-mentioned measurements, the discharge circuit was improved in order to decrease direct-current resistance and inductance as follows.

1) Capacitors were moved from the outside of vacuum chamber to the inside and arranged on the thrust stand near the PPT. Then, general-purpose polypropylene capacitors were replaced by mica capacitors with a total capacitance of 9.0 μF with both a low resistance and a low inductance.

2) In consideration of an increase of direct-current resistance due to skin effect, transmission cables with a cross-section of 0.5 mm×7 mm made of twisted copper wires of 0.05 mm in diameter were used instead of circular section cables of 2 mm in diameter made of twisted copper wires of 0.1 mm.

Table 1 shows parameters of discharge circuits before/after the improvement. Both the direct-current resistance and the inductance decreased due to the improvements. After the improvements, performances of the preliminary PPT were measured using the improved circuit. Then, some of thrust performances were significantly enhanced, e. g., thrust-to-power ratio (impulse bit per unit stored energy) was improved from 51 μN/W (μNs/J) to 71 μN/W (μNs/J), transfer efficiency from 60 % to 78 % and thrust efficiency from 8 % to 13 % with a cavity length of 34 mm and a stored energy of 14.6 J, though the specific impulse and acceleration efficiency hardly changed.

**Table 1 Parameters of discharge circuits before/after improvements**

| | Capacitance, μF | $R_{tran} + R_c$ , Ω | $L_{tran} + L_c$ , μH |
|---|---|---|---|
| Before improvement | 13.2 (max) | 0.24 | 3.9 |
| After improvement | 9.0 (max) | 0.05 | 0.35 |

## IV. Electrothermal Pulsed Plasma Thruster with a Propellant Feeding Mechanism

### A. Electrothermal PPT with a side-fed-type propellant feeding mechanism

Figure 9 shows a PPT with a propellant feeding mechanism[6, 7] designed considering the results of the preliminary PPT and Ref. 8. A cavity is formed between two PTFE bars of 6 mm in thickness and two Pyrex® glass bars of 5 mm in thickness. The cross-sectional area of the cavity (6.5 $mm^2$) is a little smaller than that of the preliminary model (7.1 $mm^2$). The cavity length is 12 mm. The PTFE bars are provided due to spring loads of approximately 3 N. The glass bars are fixed to the body. The anode and the cathode are made of tungsten and stainless steel, respectively. Main discharge is initiated by an igniter mounted in the cathode nozzle. The nozzle has a length of 28 mm and a half angle of 30 degree.

### B. Experiments and numerical simulation

The PPT showed initial performances of impulse bit per unit stored energy (thrust-to-power ratio) of 43-48 μNs/J (μN/W), specific impulse of 470-500 s and thrust efficiency of 11-12 % as shown in Fig. 10. It is remarkable that performance is kept high even at the low energy of 4.5 J.

Mass shots calculated by an unsteady numerical simulation[6,7] show excellent agreements with the experimental results. Therefore, we consider that phenomena in the cavity (generation of plasma, heat supply to the PTFE, and ablation) and the discharge circuit are well simulated with this model. The calculated impulse bits are somewhat larger than the experimental results. Other neglected factors lowering the impulse bit should be considered in a future study, e.g., flow separation from the nozzle surface.

A calculated result showed the existence of considerable amount of ablation delaying to the discharge. However, it was also shown that this phenomenon should not be regarded as the late time ablation (LTA)[9] for electrothermal PPTs because the neutral gas ablated delaying to the discharge generated most of total pressure and impulse bit.[6, 7]

A 10000-shot operation was conducted at a frequency of 0.5 Hz with a stored energy of 8.8 J corresponding to a

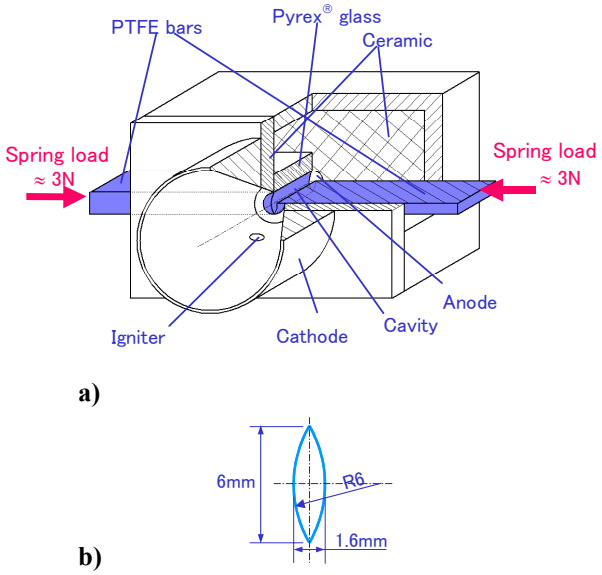


**Figure 9. Electrothermal pulsed plasma thruster with a propellant feeding mechanism: a) thruster and b) cross section of cavity.**

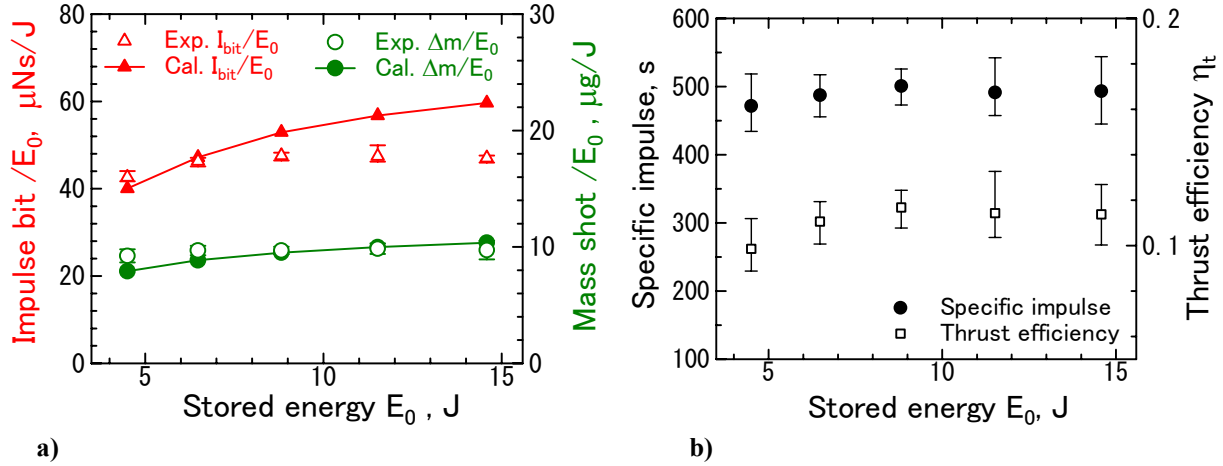


**Figure 10. Initial performance vs stored energy: a) experimental and calculated impulse bit and mass shot per unit stored energy, and b) measured specific impulse and thrust efficiency.**

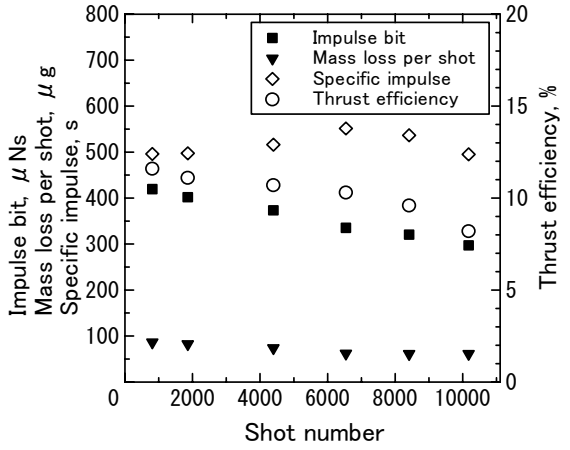


**Figure 11. Result of a repetitive 10000-shot test ($E_0$=8.8 J).**

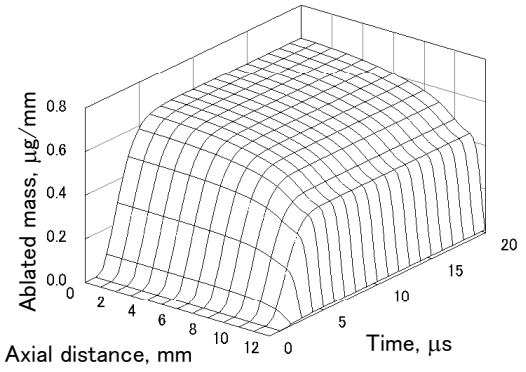


**Figure 12. Calculated time and spatial distribution of ablated mass per unit area ($E_0$=8.8 J).**

power of 4.4 W. [6,7] Figure 11 shows changes in performances during the test. Both the impulse bit and the thrust efficiency decrease gradually because of uneven receding of PTFE surface. Figure 12 shows a calculated time and spatial distribution of ablated mass per unit area. The uneven surface of the propellant depends on the axial distribution of plasma density in the cavity. In spite of the uneven ablation on the surface, each PTFE bar of approximately 2 mm was used and supplied by the propellant feeding mechanism, and a total impulse of 3.6 Ns was obtained.

## V. Effects of Nozzle Configuration on Performance

It is thought that performance of an electrothermal PPT is influenced by configuration of the nozzle, because the electrothermal PPT mainly accelerates plasma gas with aerodynamic force. In addition, it is possible that electromagnetic acceleration which may be generated due to divergent current in the nozzle is also influenced by the nozzle configuration. In present study, performances of a coaxial PPT are measured with divergent nozzles of various lengths in order to investigate their effects on thrust performances. An electrothermal PPT with a cavity of 3 mm in diameter and 19 mm in length is used for the experiment. The nozzle length is varied from 3.5 mm to 20 mm with a constant half angle of 15 degree. Cathodes with a constant diameter, i.e., nozzles with 0-degree half angle are also tested for comparison.

Figure 13 shows various performances versus nozzle length. The PPT with 15-degree nozzles showed higher performances in impulse bit per unit stored energy, specific impulse and thrust efficiency than the PPT with 0-degree nozzle. Therefore, a divergent nozzle is necessary for efficient acceleration of plasma gas in an electrothermal PPT.

As for the PPT with 0-degree nozzle, the shorter nozzle shows better performance, because momentum and energy losses due to interactions between the plasma flow and the nozzle wall, e.g. viscosity effect and surface recombination, increase with the nozzle length.

As for the PPT with 15-degree nozzle, the impulse bit gradually increased with the nozzle length, though the mass shot per unit stored energy gradually decreased with increasing the nozzle length. The reason for the tendency is thought as follows. The energy supplied into the nozzle region increases with nozzle length, because the discharge current is distributed not only in the cavity but also in the nozzle region. Then, the energy supplied into the cavity region decreases, and therefore, the ablated mass of the PTFE decreases with increasing the nozzle length. On the other hand, a longer nozzle generates more effective aerodynamic acceleration, and it is possible that the discharge current distributed in a longer nozzle generates larger electromagnetic force. As a result, the impulse bit, the specific impulse and thrust efficiency gradually increase with the nozzle length.

However, a nozzle length longer than 11 mm does not show good benefit-to-size ratio, because the difference in the performances between the 11-mm nozzle and 20-mm nozzle is not significant.

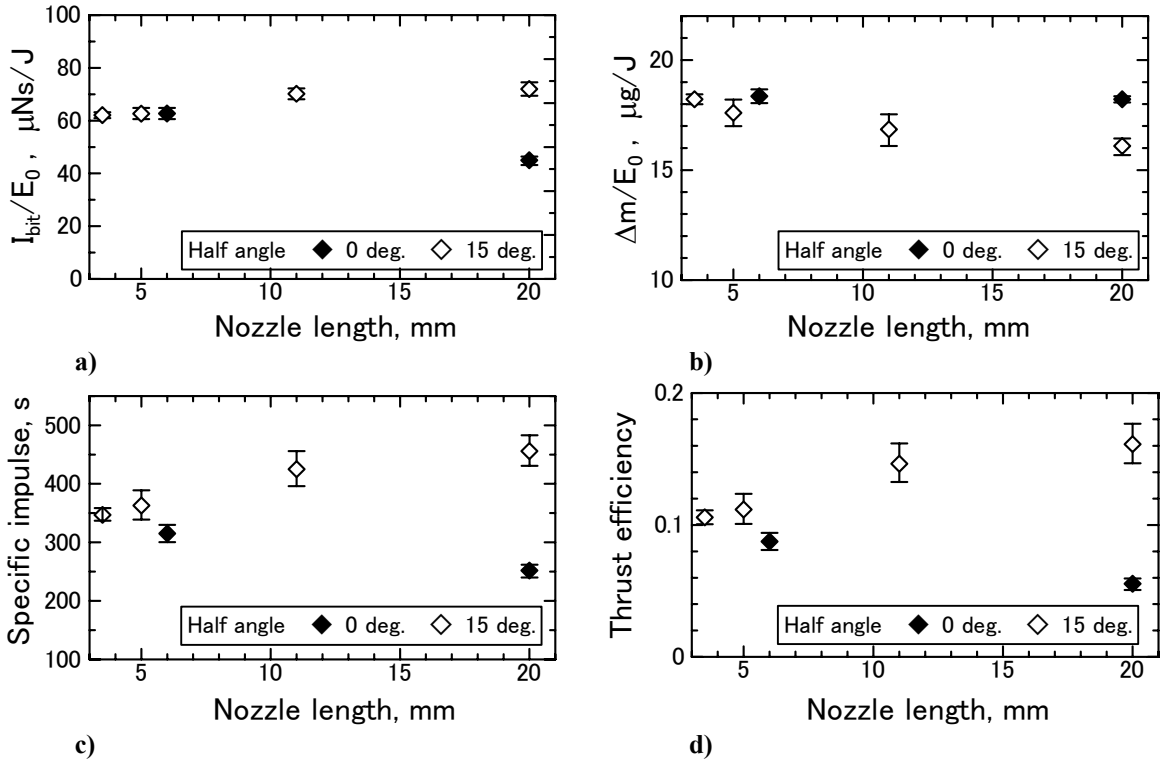


**Figure 13. Performances vs nozzle length for nozzle half angles of 0 and 15 degrees (cavity diameter: 2.5 mm): a) impulse bit per unit stored energy, and b) mass shot per unit stored energy.**

## VI. Multi-Cavity Electrothermal PPT

### A. Concept of multi-cavity electrothermal PPT

We propose a multi-cavity electrothermal PPT in order to lower the decreasing rate of impulse bit in a repetitive operation as a substitute for the propellant feeding mechanism to use a large amount of propellant. The PPT can induce discharges in a number of cavities with an igniter mounted in a nozzle.

Figure 14 shows a schematic diagram of a multi-cavity electrothermal PPT (a PPT with three cavities as an example). The PPT has a cathode and an igniter for multiple cavities and anodes. If the first discharge is generated in the cavity with the igniter, a discharge is induced in the next cavity because of a hole connecting the two cavities near the nozzle exit. Diodes as many as the cavities are used in the charging circuit in order to prevent supply of all stored energy into a cavity. Then, stored energy is evenly divided and supplied into the cavities.

Applying this mechanism to a PPT with a number of cavities, discharges can be induced in all of the cavities. Figure 15 shows a schematic diagram of a multi-cavity PPT with 24 cavities and 4 igniters as an example. In the PPT, any line consisting of 6 cavities can be discharged by selecting the igniter of the line without using any high-voltage switch.

Although impulse bit gradually decreases in a repetitive operation, the decreasing rate

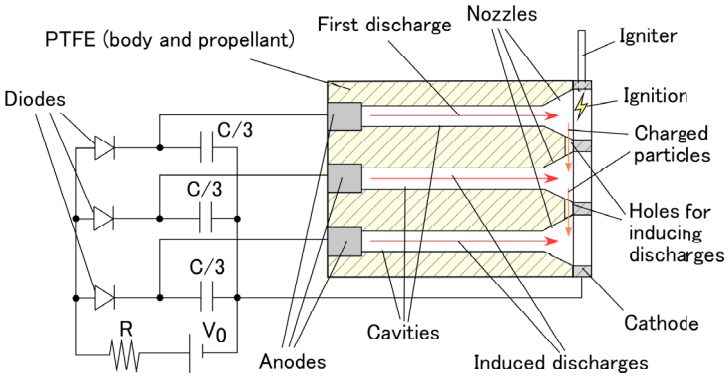


**Figure 14. Schematic diagram of a multi-cavity electrothermal PPT (a PPT with three cavities as an example).**

of the multi-cavity PPT is expected to be slower than that of a conventional PPT with a cavity, because increasing rate of the cavity diameter of the multi-cavity PPT is slower than the conventional PPT due to the lower discharge energy per cavity and lower mass shot per cavity.

In practical use, a satellite can know an impulse bit at a shot number, referring the record of impulse bit depending on shot number obtained beforehand in a repetitive operation in a grand test.

### B. Experiments

In this study, a repetitive 10000-shot operation is carried out using a PPT with two cavities and compared with a result of a conventional PPT with a cavity, and an initial operation test is carried out using a PPT with three cavities. Table 2 shows experimental conditions of the tests and initial impulse bits.

Each cavity has a length of 35 mm and a diameter of 2.5 mm, and each distance between central axes of cavities is 10 mm. Each hole for induction has a cross section of 2 mm × 3 mm. The each nozzle has a half angle of 15 degree and length of 10 mm, which is designed considering the experimental results of the chapter V in this paper. As a diode in the charging circuit, GP02-40 (Vishay Semiconductor) with reverse voltage endurance of 4 kV and maximum allowable current of 0.25 A is used. The diode has a small body of approximately 3 mm dia × 5 mm len.

Figure 16 shows discharge current waveforms of one-cavity and two-cavity PPTs measured with a Rogowski coil. This figure shows that Current waveforms of one-cavity and two-cavity PPTs measured with a Rogowski coil showed that the second discharge is induced delaying to the first

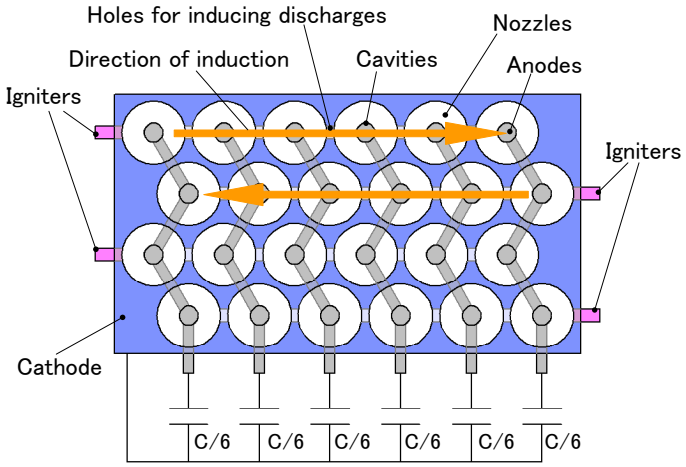


**Figure 15 Schematic of a multi-cavity PPT with 24 cavities as an example (without charging circuit).**

**Table 2 Experimental conditions and initial impulse bits**

| Number of cavities | Total stored energy | Stored energy per cavity | Initial impulse bit (total of cavities) |
|---|---|---|---|
| 1 | 14.6 J | 14.6 J | 1229 μNs |
| 2 | 14.6 J | 7.3 J | 1098 μNs |
| 3 | 14.6 J | 4.9 J | 992 μNs |

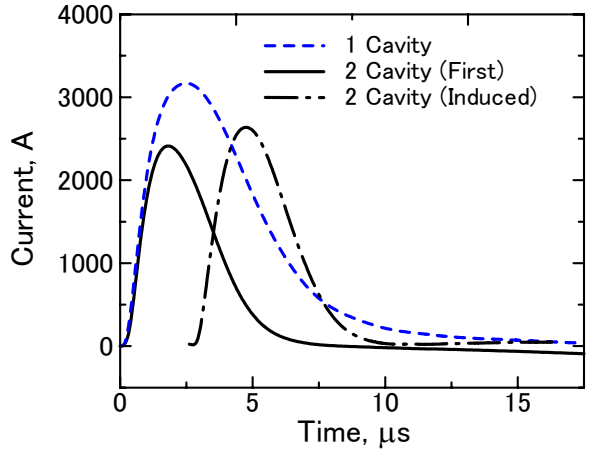


**Figure 16. Discharge current waveforms of one-cavity and two-cavity PPTs.**

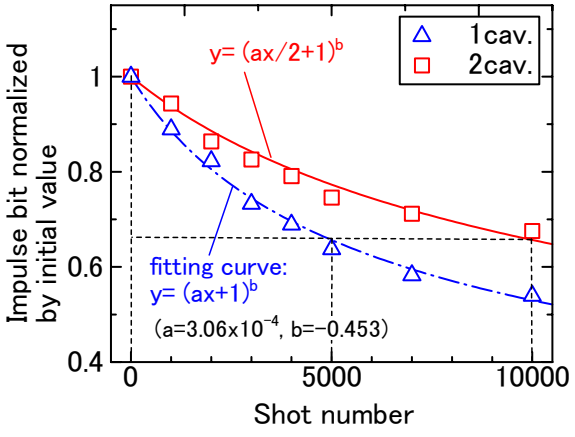


**Figure 17. Impulse bit vs shot number in 10000-shot operations with the one-cavity and two-cavity PPTs.**

discharge for approximately 2.7 μs, and that the waveform of the induced discharge has almost the same configuration as the initial discharge. The time lag between the discharges is negligible for satellites.

Figure 17 shows changes in impulse bits normalized initial values during repetitive 10000-shot operations with the one-cavity and two-cavity PPTs at a frequency of 0.5 Hz. It is shown that the rate of decrease in normalized impulse bit of the two-cavity PPT is slower than that of the one-cavity PPT, though an initial impulse bit of the two-cavity PPT is a little smaller than that of the one-cavity PPT. The shot number at which the two-cavity PPT generates a certain normalized impulse bit is approximately twice the shot number at which the one-cavity PPT generates the same normalized impulse bit. Therefore, if this relationship continues in an operation with more shots, a total impulse obtained with the two-cavity PPT will be approximately 1.8 times total impulse with the one-cavity PPT, considering that the initial impulse bit of the two-cavity PPT is about 10 % smaller than that of the one-cavity PPT.

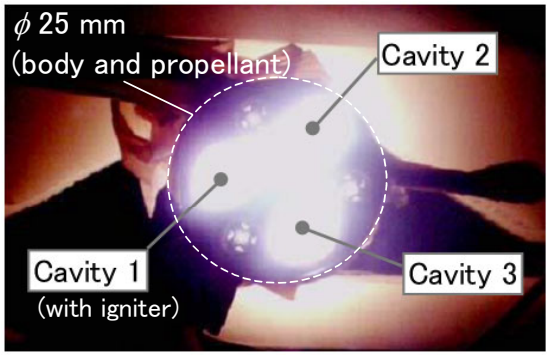


**Figure 18. Photograph of discharging three-cavity PPT.**

As a result, total impulses of 8.5 Ns and 8.7 Ns were obtained for the 10000-shot operation with the one cavity PPT and the two-cavity PPT, respectively. The diameter of the one-cavity PPT after the 10000-shot operation is nearly 7 mm as an average in the cavity. Therefore, assuming that the final diameter of the cavity is equal to the inner diameter of nozzle exit (8 mm), the maximum shot number of the one-cavity PPT is estimated as 15000 shots, and total impulse as 11.5 Ns. On the other hand, a total impulse of 20.5 Ns with a maximum shot number of 30000 shots is expected for the two-cavity PPT under the same assumption.

In the initial operation test with the three-cavity PPT, discharges were induced in all of the three cavities as shown in Fig. 18.

## VII. PPT Utilizing Electrothermal and Electromagnetic Accelerations

Electromagnetic-acceleration-type PPTs generally have higher specific impulse but lower impulse bit than electrothermal-acceleration-type PPTs. We designed and examined a PPT utilizing both electrothermal and electromagnetic accelerations in order to achieve both high thrust-to-power ratio (impulse bit per initial stored energy) and high specific impulse. Figure 19 shows a schematic diagram of the PPT, which has parallel electrodes made of copper for the electromagnetic acceleration, and a room formed with two sidewalls made of Pyrex glass and the two electrodes for raising pressure, and a divergent nozzle for aerodynamic acceleration. The nozzle has a length of 30 mm and a half angle of 20 degrees.

### A. Experiments

Impulse bit and mass shot are measured varying the distance between the electrodes *h,* the width of the exposed propellant surface *w*, and the initial stored energy. Mass losses of the grasses and the electrodes are included in mass shot as well as mass loss of the PTFE bar.

Figure 20 shows performances versus stored energy. When the distance between electrodes is 10 mm, the impulse bit per unit stored energy gradually decreases with the stored energy, though mass shot per unit stored energy gradually increases. Accordingly, both specific impulse and thrust efficiency decrease with the stored energy. Although this tendency is also observed slightly when the distance between the electrodes is 20 mm, all of performances are roughly constant.

Figure 21 shows performances versus the width of the exposed propellant surface. In each case of $h$=10 mm and $h$=20 mm, the mass shot increases with the propellant

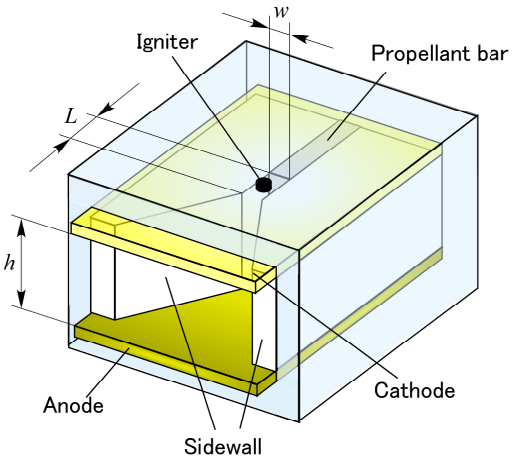


**Figure 19. Schematic diagram of a PPT utilizing electrothermal and electromagnetic accelerations.**

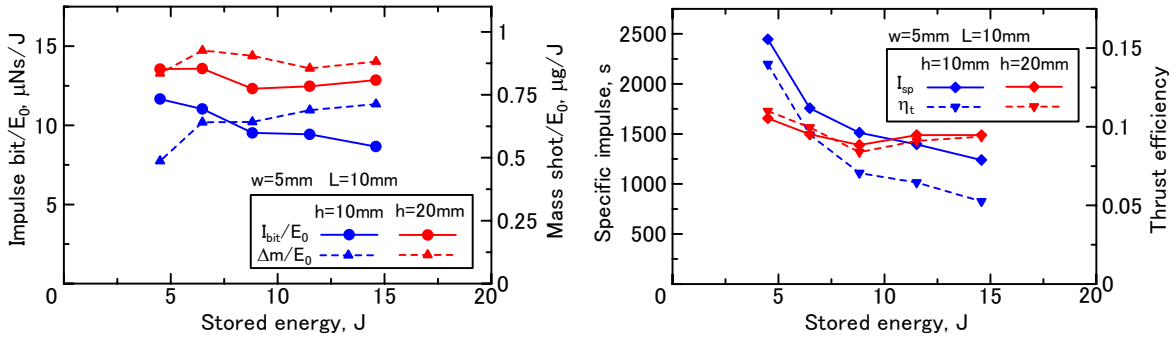


a) b)

**Figure 20. Performances vs stored energy: a) impulse bit and mass shot per unit stored energy, and b) specific impulse and thrust efficiency.**

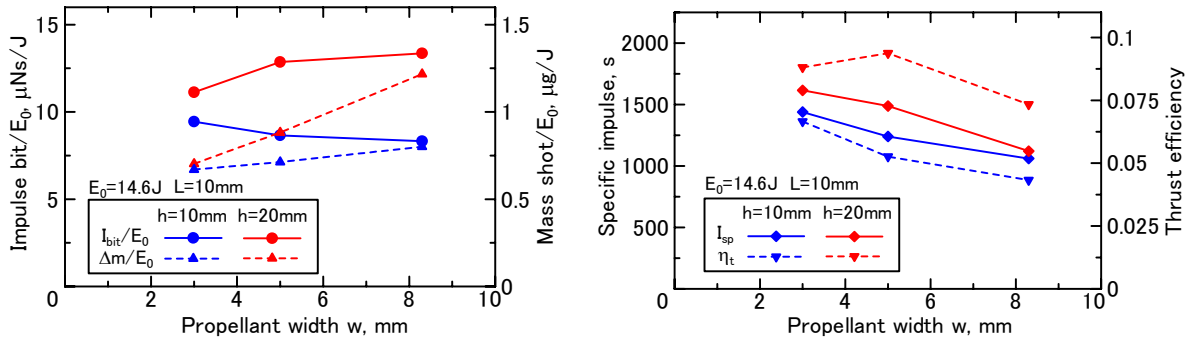


a) b)

**Figure 21. Performances vs width of exposed propellant surface: a) impulse bit and mass shot per unit stored energy, and b) specific impulse and thrust efficiency.**

width because the exposed propellant area increases, though the impulse bit does not considerably change because pressure decreases. Therefore, higher specific impulse and higher thrust efficiency are obtained for the configuration with a smaller propellant width. It is also shown that the performance is improved with a long distance between the electrodes because of high transfer efficiency due to high equivalent plasma resistance.

Figure 22 shows impulse bit per unit exposed propellant area ($I_{bit}/A$) versus the aspect ratio of the exposed propellant surface. The aspect ratio $A_R$ is defined as $h/w$. As a result, within the experimental conditions in this study, it is shown that the impulse bit per unit exposed propellant area is proportional to the aspect ratio if the distance between electrodes is fixed.

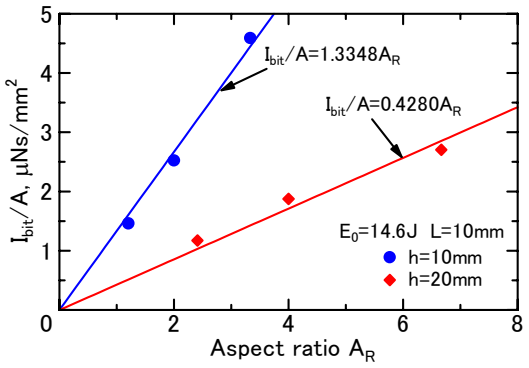


**Figure 22. Impulse bit per propellant surface area vs aspect ratio of the surface.**

The thrust-to-power ratios obtained with the configurations in this study are not greatly improved compared with a conventional electromagnetic PPT. It is necessary to decrease the volume of $w \times h \times L$ in order to obtain the higher pressure. In addition, there is a possibility that the impulse bit increases if external magnetic field with the decelerating direction considering the Lorentz force is applied by permanent magnets in the region within the distance of $L$ from the propellant surface, and external magnetic field with the accelerating direction in the nozzle region.

## VIII. Summary of Initial Performances of Electrothermal PPTs in Osaka University

Figure 23 shows impulse bit per unit stored energy versus specific impulse of the electrothermal PPTs in Osaka University (initial performances) as a summary. Both the maximum thrust efficiency of 17.4 % and thrust-to-power ratio of 84.2 μN/W were obtained with the configuration of multi-cavity PPT when the stored energy of 14.6 J is supplied into a cavity. It is because the multi-cavity PPT has the smallest cross-sectional area of 4.9 $mm^2$. That is, with decreasing cross-sectional area of cavity, transfer efficiency increases, and then, acceleration efficiency increases because pressure in the cavity increases.

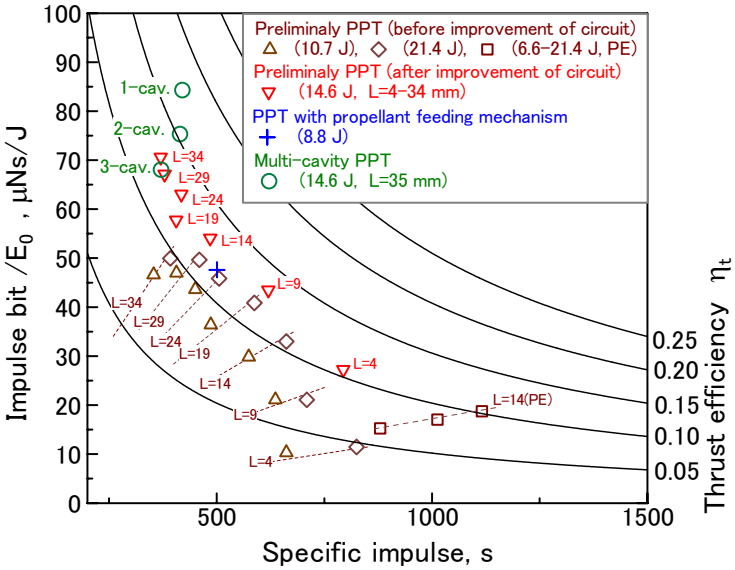


**Figure 23. Impulse bit per unit stored energy (thrust-to power ratio) vs specific impulse of electrothermal PPTs in Osaka University (initial performances).**

## IX. Conclusions

The main results were as follows.

*Preliminary study*

1) A small cross-sectional area of a discharge cavity improved the performance, because it decreases transmission energy loss in the discharge circuit due to high plasma resistance in the cavity and increases pressure in the cavity.
2) There was an optimum cavity length for thrust efficiency, because a short cavity increases transmission energy loss in the discharge circuit and a long cavity increases acceleration energy loss in the PPT.

*PPT with propellant feeding mechanism*

3) A PPT with a propellant feeding mechanism showed initial performances of impulse bit per unit stored energy (thrust-to-power ratio) of 43-48 μNs/J (μN/W), specific impulse of 470-500 s and thrust efficiency of 11-12 % with stored energy of 4.5-14.6 J.
4) The performances calculated with an unsteady numerical simulation approximately agreed with measured initial performances.
5) A calculated result showed the existence of considerable amount of ablation delaying to the discharge. However, it was also shown that this phenomenon should not be regarded as the LTA for electrothermal PPTs because the neutral gas ablated delaying to the discharge generates most of total pressure and impulse bit.
6) A total impulse of 3.6 Ns was obtained in a repetitive 10000-shot operation with a stored energy of 8.8 J per shot. However, both the impulse bit and the thrust efficiency decreased gradually because of uneven receding of PTFE surface. The uneven surface of the propellant after the repetitive operation was qualitatively explained with the calculation.

*Effects of nozzle configuration on performance*

7) As for the electrothermal PPT with 15-degree nozzle, almost no difference in impulse bit by nozzle lengths is shown. A longer nozzle does not have good benefit-to-size ratio, because the difference in the performances is considerably small.

*Multi-cavity PPT*

8) The decreasing rate of the two-cavity PPT was slower than that of a conventional PPT with a cavity.
9) The three cavity PPT was successfully operated. It was suggested that this mechanism of inducing discharges in multiple cavities is applicable to a PPT with more cavities for a higher total impulse.

*PPT utilizing electrothermal and electromagnetic accelerations*

1) A higher specific impulse and a higher thrust efficiency are obtained with a configuration of a smaller propellant width and a longer distance between the electrodes.

## References


[1] Burton, R. L., and Turchi, P. J., "Pulsed Plasma Thruster," *Journal of Propulsion and Power*, Vol. 14, No. 5, 1998, pp. 716-735

[2] Edamitsu, T., Tahara, H., and Yoshikawa, T., "Performance Characteristics of a Coaxial Pulsed Plasma Thruster with PTFE Cavity," *Proc. Asian Joint Conferences on Propulsion and Power 2004*, March 2004, p. 324-334.

[3] Edamitsu, T., Tahara, H., and Yoshikawa, T., "Effects of Cavity Length and Material on Performance Characteristics of a Coaxial Pulsed Plasma Thruster," *24th International Symposium on Space Technology and Science*, Paper ISTS-2004-b-6, June 2004.

[4] Rysanek, F., and Burton, R. L., "Performance and Heat Loss of a Coaxial Teflon Pulsed Thruster," *27th International Electric Propulsion Conference,* Paper IEPC-01-151, Oct. 2001.

[5] Burton, R. L., Wilson, M. J., and Bushman, S. S., "Energy Balance and Efficiency of the Pulsed Plasma Thruster," AIAA Paper 98-3808, July 1988.

[6] Edamitsu, T., Tahara, H., and Yoshikawa, T. "Performance Measurement and Flowfield Calculation of a Pulsed Plasma Thruster with a PTFE Cavity," *Asian Joint Conference on Propulsion and Power 2005*, Paper AJCPP2005-22083, Jan. 2005.

[7] Edamitsu, T., and Tahara, H, "Performance Measurement and Flowfield Calculation of an Electrothermal Pulsed Plasma Thruster with a Propellant Feeding Mechanism," *29th International Electric Propulsion Conference*, Paper IEPC-05-105, Nov. 2005.

[8] King, D. M., Solomon, W. C., Carroll, D. L., Burton, R. L., Antonsen, E. L., Rysanek, F., Frus, J., "Development of a Multiplexed Coaxial Pulsed Plasma Thruster," *27th International Electric Propulsion Conference,* Paper IEPC-01-150, Oct. 2001.

[9] Mikellides, P. G., and Turchi, P. J.: Modeling of Late-Time Ablation in Teflon Pulsed Plasma Thrusters, AIAA Paper 96-2733, 1996.